Spontaneous-fission half-lives for even nuclei with $Z \geq 92$†

J. Randrup*
Lawrence Berkeley Laboratory, University of California, Berkeley, California 94720

S. E. Larsson, P. Möller, and S. G. Nilsson
Department of Mathematical Physics, Lund Institute of Technology, Lund, Sweden

K. Pomorski
Institute of Physics, Maria Sklodowska-Curie University, Lublin, Poland

A. Sobiczewski
Institute for Nuclear Research, Hoza 69, PL—00681 Warszawa, Poland
(Received 22 September 1975)

The spontaneous-fission process for doubly even nuclei with $Z \geq 92$ is studied in a semiempirical WKB framework. One-dimensional fission barrier potentials are established from theoretical deformation-energy surfaces based on the droplet model and the modified-oscillator model. The effects of axial asymmetry as well as reflection asymmetry have been taken into account. Macroscopic (irrotational flow) inertial-mass functions and alternatively microscopic (cranking model) inertial mass parameters have been employed for the calculation of the fission half-lives. With one over-all normalization parameter it is possible to fit the experimental half-lives to within a factor of 20 on the average. The resulting effective inertial-mass functions are used to estimate the stability of the transactinide elements. Only minor differences with previous estimates for the r process and superheavy nuclei are encountered.

[NUCLEAR STRUCTURE Even nuclei with $Z \geq 92$; calculated sf $T_{1/2}$.]

I. INTRODUCTION

Since an earlier semiempirical study[1] of the spontaneous-fission process for transthorium elements, improved theoretical deformation-energy surfaces have been obtained,[2] based on the modified-oscillator single-particle model[3] and the macroscopic droplet model.[4] In those calculations the effect of axial asymmetric distortions as well as reflection asymmetric distortions are included in a more accurate way.

On the basis of new calculational material, we consider in this paper the even-even elements beyond thorium, for the purpose of clarifying the accuracy of the theoretical calculations of the spontaneous-fission half-lives. The investigation follows the lines of the semiempirical method introduced in Ref. 1. Let us briefly outline the general approach.

The fission process is treated as a penetration through a one-dimentional potential barrier, calculated along an effective path in the multidimensional deformation space. The penetrability is calculated in the WKB approximation. Thus one needs the action integral K along the fission path,

$$K = \frac{2}{\hbar} \int_{r_1}^{r_2} [2B(r)(V(r) - E_{\text{vib}})]^{1/2} dr \,. \tag{1}$$

The path is described by the fission coordinate r. $V(r)$ is the deformation energy of the shape described by r and $B(r)$ is the effective inertial-mass function corresponding to a motion along the fission path. Moreover, E_{vib} denotes the fission-mode zero-point energy in the initial state; it is taken to 0.5 MeV, following Ref. 3. The integral limits r_1 and r_2 are the entrance and exit points, respectively. From the integrated action K the half-life $T_{1/2}$ is given by the relation[3]

$$T_{1/2} = 10^{-28.04} \times (1 + e^K) \text{ yr} \,. \tag{2}$$

The fission barrier potential $V(r)$ is calculated theoretically. In the present study, $V(r)$ is based on recent calculations presented in Ref. 2, as will be described in Sec. II.

As present the theoretical calculations of the effective fission inertial-mass function $B(r)$ are less accurate than the calculations of the potential $V(r)$. Therefore we introduce one over-all mass-renormalization parameter which is subsequently determined by fitting to the known half-lives. In this paper two trial forms of $B(r)$ are studied. One is based on macroscopic (hydrodynamical) irrotational-flow calculations and is similar to what was previously studied.[1,5] In addition to this, we have calculated microscopic inertial-mass parameters in the cranking approximation and used these for

the determination of the effective fission inertia. This will be described in Sec. III.

In Sec. IV the established fission barrier potentials are used to determine the effective inertial-mass functions. Subsequently, calculations are made of the stability of so far unobserved heavier nuclei.

II. THE THEORETICAL FISSION BARRIER POTENTIALS

According to the semiempirical method introduced in Ref. 1, the fission barrier potential is generated from the stationary points on the deformation-energy surface (i.e., the minima and saddle points) together with one (or more) additional point(s) in the exit region beyond the last saddle point.

The theoretical fission barrier potentials employed in the present study are based on the deformation-energy surfaces underlying Ref. 2. In these calculations the macroscopic part of the deformation energy is given by the droplet model[4] with the shape functions B_s, B_c, B_r, B_v, and B_w obtained by exact numerical integration in the ϵ parametrization. The microscopic part of the energy is based on the Strutinski shell-correction method[6] applied to the modified-oscillator model[3]; the potential parameters are those denoted "$A = 242$" in Ref. 3, and the pairing strength is assumed independent of deformation.

The basic calculation of the deformation-energy surfaces was performed in the $(\epsilon\epsilon_4)$ space. In addition to the quadrupole (ϵ) and hexadecapole (ϵ_4) deformations other types of deformation have been taken into account as well, as is briefly described in the following. This part of the study follows closely that of Ref. 7 and more details may be found there.

A. Axial asymmetry

We have included the effect of axially asymmetric nuclear shapes as described by the γ deformation coordinate. A detailed study of the γ deformations in the actinide region is performed in Ref. 8 and a similar study for the superheavy region is performed in Ref. 9. Here we put the emphasis on the most recent results employing a three-dimensional variation in the $(\epsilon\epsilon_4\gamma)$ space.

The calculation of the γ deformation energies are refined relative to Ref. 8 by taking into account the complete couplings between shells N, $N \pm 2$, $N \pm 4$, etc. Moreover, we have used an extended version of the droplet model code which includes axially asymmetric shapes.[10]

In the actinide and transactinide region the first saddle point exhibits an instability with respect to γ distortions. The corresponding γ reduction of the saddle-point energy is mainly a neutron effect in that domain. As can be seen from Fig. 1, the onset of the axial asymmetry occurs roughly at neutron number $N = 140$ and the maximum effect is obtained at $N = 150$–152. Very similar results were obtained by Pashkevich[11] and later on also by Götz *et al.*[12] using a Woods-Saxon type potential.

The γ instability can be understood in terms of mixings of specific single-particle orbitals having particularly large matrix elements of the asymmetry operator. This operator couples only states in the same shell with $\Omega' = \Omega \pm 2$ and $n_2' = n_2$. The corresponding matrix elements are given by

$$\langle n_\perp, \Lambda + 2 \,|\, (x + iy)^2 \,|\, n_\perp, \Lambda \rangle = [n_\perp(n_\perp + 2) - \Lambda(\Lambda + 2)]^{1/2} . \tag{3}$$

In Fig. 2 the neutron orbitals, characterized on the prolate side by their asymptotic quantum numbers $[Nn_z\Lambda\Omega]$, are plotted along the γ direction for fixed $\epsilon = 0.40$ and $\epsilon_4 = 0.040$. It is seen that some strongly interacting orbitals bend convexly away from each other. Most of these orbitals are situated around neutron number $N = 150$. Hence, for this neutron number a gap is obtained with increasing γ deformation. The mutual repulsion of the interacting orbitals, which are originally rather closely spaced, causes a decrease in the level density which in turn gives rise to a reduced shell-correction energy.

A further study of Fig. 2 suggests that the barrier between the ground state and the isomeric minimum (located at approximately $\epsilon = 0.40$) should be γ unstable for nuclei with $Z = 84$–86 and $N \approx 120$. In fact, there is found a considerable reduction of the barrier due to axial asymmetry.[13]

B. Reflection asymmetry

In the nuclear region considered here, reflection asymmetric shapes play an important role for large nuclear distortions. For our present study we have employed the reflection-asymmetry corrections to the second saddle point given in Ref. 14. They were obtained by calculating a two-dimentional map using a combined asymmetrical coordinate ϵ_{24} and a combined asymmetrical coordinate ϵ_{35}.

It should be added here that these calculations,[14] as well as calculations with the folded-Yukawa model,[15] suggest that the second barrier for some uranium and plutonium isotopes is split into two humps separated by a shallow minimum. We have taken this into account by adding to the usual five characteristic points two additional ones corresponding to the third minimum and the third saddle point.

The reflection asymmetry also plays a role beyond the last saddle point by significantly lowering the fission valley bottom relative to that pertaining to purely symmetric shapes. Following Ref. 1 we chose the last point characterizing the fission barrier to have $\epsilon = 1.0$ and $\epsilon_4 = 0.140$. The importance of the reflection asymmetry has been studied. A neglect of the asymmetry in the exit region leads to an incorrect isotopic variation of the calculated half-lives (cf. Ref. 7). Therefore, we have for each nucleus chosen that value of the asymmetry coordinate ϵ_{35} which leads to the lowest energy. This improves the fit to the experimental half-lives considerably, by a factor of almost 10 on the average.

C. Hexäkontatettarapole ground-state deformations

We have also studied the effect of P_6 deformations at the ground-state minimum. The P_6 deformation energies used are those given in Ref. 2. Most of the nuclei considered have some P_6 deformation in the ground state, and it turns out that the inclusion of the correction improves the overall fit to experiment by a factor of around five. For this reason we have included this effect in the employed fission barriers.

As described in Ref. 1, a one-dimensional fission barrier potential is established by first transforming the characteristic points from the multi-dimensional deformation space into a single fission coordinate r. Subsequently, appropriate polynomials are spliced through the transformed points.

For the fission coordinate r the equivalent center-of-mass separation is used, i.e., the separation between the two fragments created by a cut through the center of mass. In the calculation of r the effect of reflection asymmetry is neglected. It should be pointed out, however, that the effect of P_4 (but not P_6) deformations *is* included. This has not been done previously. It has a large bearing on the value of r for large nuclear distortions. When ϵ_4 is taken into account the value of r is usually reduced. As far as the fit to known fission half-lives is concerned, this effect of ϵ_4 on r can, to a large part, be compensated by an increase in the effective fission inertia. But as far as predictions for nuclei with less extended barriers, such as most of the superheavy nuclei or the r-process nuclei, the effect will be significant, giving rise to an increase in the predicted half-life. In Sec. IV previous predictions[24] are re-examined in light of this effect.

Before calculating the penetration integral (1) we have added at the ground state a zero-point vibrational energy of $E_{\text{vib}} = 0.5$ MeV, in accordance with Ref. 3.

In Table I we show, for the nuclei used in the fit, the resulting values of the coordinate r and the potential V, for the characteristic points cor-

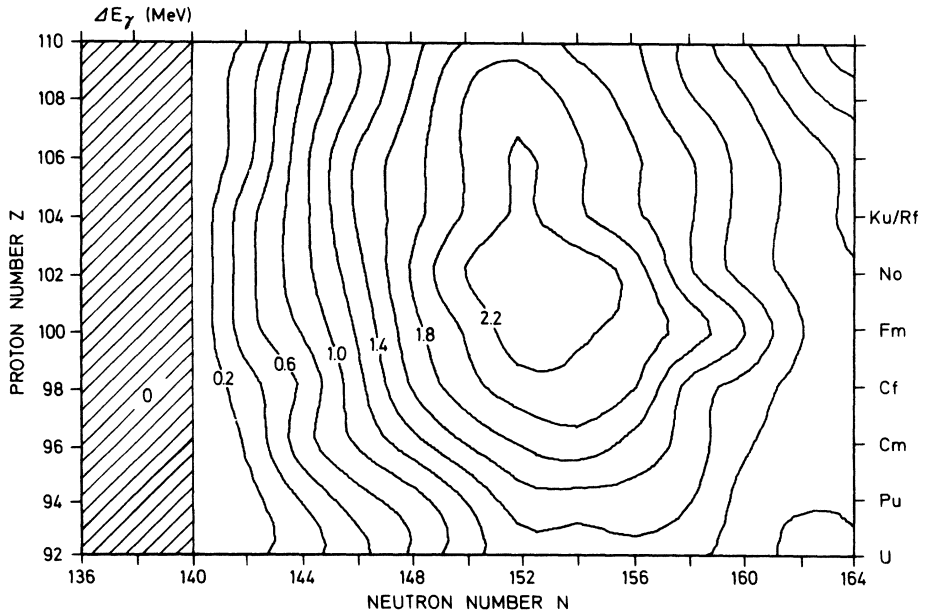

FIG. 1. Contour plot of the barrier reduction $\Delta E\gamma$ (MeV), due to the axial asymmetry, as a function of N and Z. Note that the largest reduction occurs in the vicinity of $N = 152$ and $Z = 102$.

responding to the first minimum (I), the first saddle point (A), the second minimum (II), and the second saddle point (B). When appropriate the third minimum (III) and the third saddle point (C) are also included. For purposes of illustration we have displayed in Fig. 3 a few examples of the final fission barrier potentials in terms of the r coordinate.

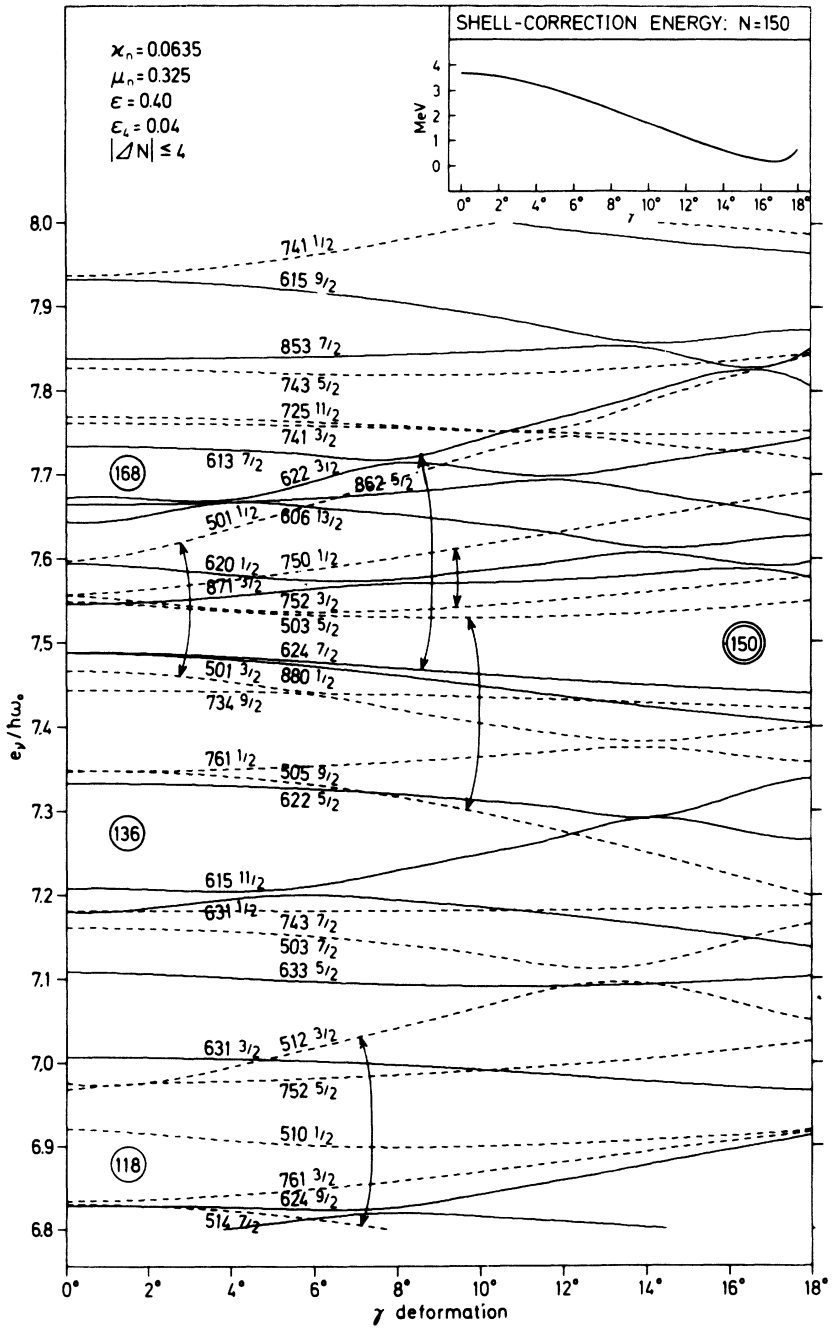

FIG. 2. Single-neutron levels in the actinide region appropriate to the first saddle point ($\epsilon = 0.40$, $\epsilon_4 = 0.04$) as a function of the axial-asymmetry coordinate γ. The arrows indicate strongly interacting orbitals. In the upper right corner, the shell-correction energy (without the pairing contribution) is shown for neutron number 150.

TABLE I. The stationary points of the deformation-energy surfaces for the nuclei included in the study. The value of the r coordinate (in units of the nuclear radius) and the deformation energy V (in MeV) is shown for the minima (I, II, III) and saddle points (A, B, C).

Z	A	r_I	V_I	r_A	V_A	r_{II}	V_{II}	r_B	V_B	r_{III}	V_{III}	r_C	V_C
92	232	0.85	−1.300	1.06	3.050	1.17	1.460	1.36	4.390	1.45	4.120	1.58	5.560
92	234	0.86	−1.620	1.05	3.380	1.17	1.290	1.40	4.490	1.48	4.000	1.59	5.020
92	236	0.86	−1.760	1.04	3.760	1.17	0.160	1.39	4.630	1.51	3.660	1.61	4.400
92	238	0.87	−1.800	1.03	4.140	1.17	0.440	1.37	4.690	1.54	3.240	1.63	3.710
94	236	0.86	−1.980	1.05	3.310	1.17	0.200	1.39	3.040	1.51	2.310	1.59	3.220
94	238	0.86	−2.130	1.04	3.680	1.17	−0.310	1.39	3.230	1.53	1.900	1.61	2.660
94	240	0.87	−2.250	1.04	4.060	1.17	−0.030	1.39	3.350	1.54	1.480	1.63	1.920
94	242	0.87	−2.390	1.09	4.310	1.17	0.340	1.37	3.360	1.59	0.920	1.66	1.140
94	244	0.87	−2.785	1.01	3.390	1.18	0.710	1.36	3.400				
96	240	0.87	−2.773	1.04	2.960	1.17	−0.890	1.38	1.670				
96	242	0.87	−3.121	1.04	3.050	1.17	−0.600	1.37	1.860				
96	244	0.88	−3.342	1.02	3.010	1.18	−0.280	1.36	2.040				
96	246	0.88	−3.385	1.01	2.970	1.19	0.060	1.36	1.970				
96	248	0.88	−3.323	1.01	2.880	1.23	0.160	1.36	1.480				
96	250	0.88	−3.058	1.01	2.700	1.25	0.090	1.36	1.660				
98	246	0.88	−3.896	1.02	2.620	1.19	−1.110	1.36	.290				
98	248	0.88	−3.985	1.01	2.540	1.24	−0.890	1.36	.390				
98	250	0.88	−3.977	1.01	2.430	1.26	−0.890	1.38	.340				
98	252	0.88	−3.741	1.01	2.330	1.27	−1.050	1.38	.150				
98	254	0.88	−3.399	1.02	2.300	1.27	−1.290	1.44	−.070				
100	244	0.87	−3.352	1.03	2.710	1.18	−2,470	1.33	−1.300				
100	246	0.88	−3.882	1.02	2.680	1.19	−2.280	1.35	−1.460				
100	248	0.88	−4.256	1.01	2.390	1.25	−2.070	1.36	−1.340				
100	250	0.89	−4.420	1.01	2.270	1.26	−2.030	1.38	−1.260				
100	252	0.89	−4.467	1.01	2.040	1.27	−2.070	1.40	−1.320				
100	254	0.88	−4.278	1.01	2.010	1.27	−2.250	1.42	−1.520				
100	256	0.88	−3.967	1.02	1.960	1.32	−2.510	1.45	−1.850				
100	258	0.88	−3.696	1.02	1.950	1.33	−3.010	1.47	−2.360				
100	260	0.88	−3.458	1.03	2.060	1.34	−3.650	1.49	−2.830				
100	262	0.88	−3.165	1.04	2.250	1.35	−4.460	1.51	−3.430				
100	264	0.87	−2.657	1.05	2.360	1.35	−5.260	1.51	−4.040				
102	252	0.88	−4.564	1.01	1.660	1.28	−3.280	1.38	−2.980				
102	254	0.89	−4.692	1.01	1.590	1.30	−3.330	1.39	−3.080				
102	256	0.88	−4.567	1.01	1.440	1.32	−3.570	1.41	−3.390				
102	258	0.88	−4.249	1.02	1.480	1.33	−3.900	1.44	−3.760				

III. THE EFFECTIVE INERTIAL-MASS FUNCTIONS

For the calculation of the spontaneous-fission half-lives we have employed two types of trial inertial-mass functions. One is based on macroscopic (hydrodynamical) calculations and is similar to what was previously employed.[1] The other is based on calculated microscopic (cranking model) inertial-mass parameters. The final results are relatively similar. We shall discuss below the two cases separately.

A. Macroscopic inertial-mass functions

Following Ref. 1, we employ a one-parameter trial inertial-mass function of the form

$$B_r^{\text{micro}} = B_r^{\text{rigid}} + k(B_r^{\text{irrot}} - B_r^{\text{rigid}}), \tag{4}$$

where B_r^{rigid} is the inertial mass associated with a rigid separation of the two fragments and B_r^{irrot} is the hydrodynamical inertial mass corresponding to irrotational flow during the fission process. The renormalization constant k is a measure of the nonirrotational flow associated with motion along the fission path.

For convenience we use a simple analytical approximation to B_r^{irrot} (an exponential). The explicit form of the macroscopic-type trial inertial-mass function thus becomes

$$B_r^{\text{macro}}(r) = 1 + k\frac{17}{15}\exp\left[\frac{c}{\lambda}(\tfrac{3}{4} - r)\right] . \tag{5}$$

Here r is measured in units of the nuclear radius $R = r_0 A^{1/3}$ and B_r^{macro} is measured in units of μ, the

reduced mass of the final two-fragment system (which we assume to be symmetrical). Moreover, λ is a numerical constant equal to 1/2.452 determined from a fit to the exact curve[16] for B_r^{irrot}.

In addition to the renormalization parameter k we have introduced a second parameter c governing the slope of the mass function. For $k=c=1$ the irrotational-flow inertial-mass function is approximately reproduced.

The study of the effect of including the various refinements in the barriers, discussed in Sec. II was performed with the macroscopic-type inertial-mass function with c kept equal to unity. In Sec. IV we shall discuss the effect of varying the slope parameter c.

B. Microscopic inertial-mass functions

As an alternative, we have calculated the spontaneous-fission half-lives on the basis of inertial-mass parameters calculated in the cranking approximation.

For the present semiempirical study we have only considered the $B_{\epsilon\epsilon}$ component of the full inertial-mass tensor. A more complete study, based on calculations of inertia tensor components within the $(\epsilon\epsilon_4\gamma)$ space, is in progress.[17]

The mass parameter $B_{\epsilon\epsilon}$ is calculated in the adiabatic cranking approximation.[18] In the BCS approximation, including the coupling to pairing vibrations, the expression for $B_{\epsilon\epsilon}$ is[19]

$$B_{\epsilon\epsilon}=2\hbar^2\left[\sum_{\nu\mu}\frac{\langle\nu\,|\,\partial H/\partial\epsilon\,|\,\mu\rangle^2(u_\nu v_\mu+u_\mu v_\nu)^2}{(E_\nu+E_\mu)^3}+P_{\epsilon\epsilon}\right]. \tag{6}$$

Here H is the single-particle Hamiltonian, in the present case the modified-oscillator Hamiltonian with the $A=242$ parameters.[3] Furthermore, u_ν and v_ν are the BCS variational parameters and E_ν is the energy of the quasiparticle state $|\nu\rangle$. The term $P_{\epsilon\epsilon}$ contains the contribution from couplings to the pairing vibrations. The total mass parameter is a sum of a proton and a neutron contribution, $B_{\epsilon\epsilon}=B_{\epsilon\epsilon}^{(p)}+B_{\epsilon\epsilon}^{(n)}$. Couplings between all oscillator shells, appearing for $\epsilon_4\neq 0$, are taken into account in the calculations.

The mass parameters obtained in this way are equivalent to the parameters calculated in a slightly different way.[20,21] In the latter calculations, one starts from the multipole moments of the nucleus as the collective variables and subsequently projects them onto the deformation parameter ϵ. The equivalence is obtained by including a sufficiently large number of multipole moments in the projection.[22]

The basic calculation of $B_{\epsilon\epsilon}$ is carried out for a 70-point grid in $(\epsilon\epsilon_4)$ space. This is sufficient to get a good approximation to $B_{\epsilon\epsilon}$ in the region of interest (except in a few cases of very large deformation). The microscopic-type trial inertial-mass function is then given by

$$B_r^{\text{micro}}(r)=\rho B_{\epsilon\epsilon}(\epsilon,\epsilon_4)\left[\frac{\partial\epsilon}{\partial r(\epsilon,\epsilon_4)}\right]^2. \tag{7}$$

The last factor, which gives the approximate transformation to the r-coordinate matrix, is evaluated along an average fission path.

One adjustable parameter is introduced in this case in the form of the overall renormalization factor ρ. One should bear in mind that because of the approximate treatment of the inertial matrix one cannot expect ρ to come out exactly equal to unity, even if the basic inertial-mass parameters were correct. On the other hand, since the adopted treatment is expected to include the main part of the inertia, the factor ρ should not be too different from unity. Recalling the empirical finding that the microscopically calculated mass parameters in the rotational case tend to come out somewhat too large, it appears satisfactory that the best fit is obtained for $\rho=0.80$.

In Fig. 4, we display as an illustration the determined effective inertial-mass functions for the same four nuclei as in Fig. 3. The solid smooth curves are the best hydrodynamical-type mass functions corresponding to $k=11.5$ and $c=1.0$. The dashed smooth curve corresponds to the best fit obtained with half the irrotational-flow slope, namely $c=0.5$. The wiggly curves represent the effective microscopic-type inertial-mass functions (with $\rho=0.80$). When comparing these different mass functions one should bear in mind that they

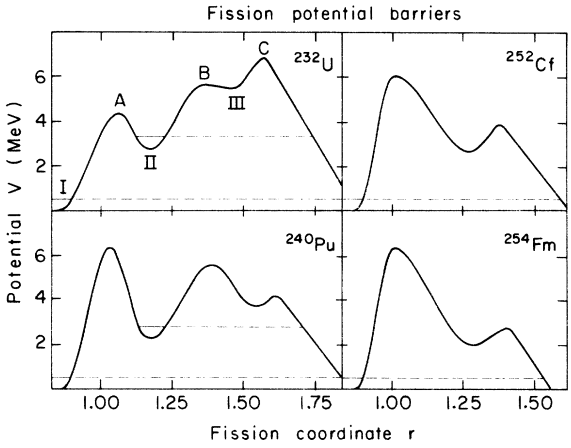

FIG. 3. Fission potential barriers for four selected nuclei, as obtained by splining polynomials through the five (or seven) characteristic points (namely the stationary points I, A, . . . plus one additional point X beyond the last saddle).

do not necessarily lead to identical half-lives for each individual nucleus. Rather, each set leads to a best overall reproduction of the experimental half-life data.[23]

IV. RESULTS AND DISCUSSION

A. The experimentally known region

With the fission barrier potentials established as described in Sec. II we have, using the different sets of trial inertial-mass functions described in Sec. III calculated the spontaneous-fission half-lives for the known even-even nuclei ranging from ^{232}U to ^{258}No. (The theoretical deformation energies for the known isotopes of element 104 are not very accurate and we have excluded this element from the test group. This exclusion should also be seen in the light of the present disagreement between reported half-lives for isotopes of this element.) Minimization of the average logarithmic deviation Δ of the calculated half-lives from the experimental ones determines, for each set of inertial functions, the adjustable parameter(s) entering the trial functions. (For collection of recent half-life data see Refs. 23–25.)

1. Macroscopic inertias

For the hydrodynamic-type inertial-mass function with $c=1$ the best reproduction of experimental half-lives is obtained for $k=11.5$. This value is larger than the previously[26] employed value of 10.0 This change is mainly due to the inclusion of the ϵ_4 dependence of the r coordinate; cf. our discussion of this point in Sec. II. The average logarithmic deviation is $\Delta=1.7$, which corresponds to a factor of around 50.

In Fig. 4 the solid curves indicate these effective mass functions. The half-lives obtained with this set of effective mass functions are shown in Fig. 5, together with the experimental data.

In agreement with the results of our earlier study[5] based on an older set of barriers, it turns out that a simultaneous variation of the slope parameter c appearing in the inertial-mass function leads to a better fit. In a contour plot of the quantity Δ as a function of k and c there is a valley passing approximately through the points ($k=11.5$, $c=1.0$) and ($k=6.5$, $c=0.5$). The variation of Δ in the direction perpendicular to the valley is rapid while along the valley the slope is rather gentle. The absolute minimum is located around ($k=6.5$,

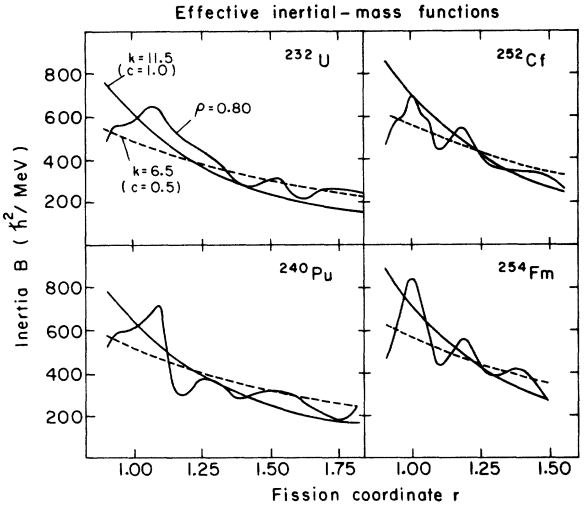

FIG. 4. Effective fission inertial-mass functions for the same four nuclei as in Fig. 3. The solid smooth curve ($k=11.5$, $c=1.0$) is the best macroscopic inertial function with c fixed to unity. The dashed curve ($k=11.5$, $c=0.5$) results (approximately) if c is also allowed to vary in the fit. The best microscopic inertial-mass function has $\rho=0.80$ and is indicated by the solid wiggly curve.

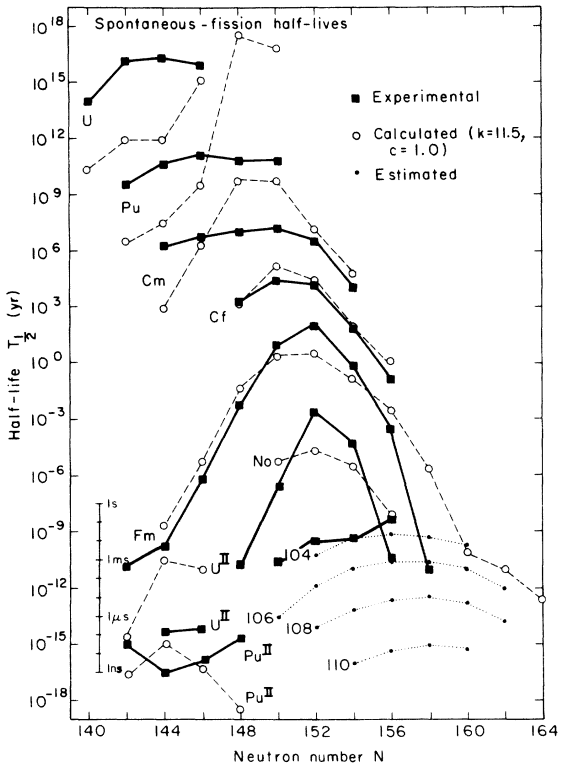

FIG. 5. Spontaneous-fission half-lives calculated with the macroscopic inertial-mass functions having $k=11.5$ and $c=1.0$ (open circles joined by dashed lines). The experimental values are indicated by solid squares joined by solid lines. In the lower left corner are included some isomeric half-lives. Also included in the figure are the half-lives calculated with the estimated approximate barriers for the transuranium elements (dots joined by dotted lines).

$c = 0.5$), with an average deviation of $\Delta = 1.4$, corresponding to approximately a factor of 25. In Fig. 4 this set of inertial functions is indicated by the dashed lines.

For a smooth inertial function, with two trial parameters governing normalization and slope, respectively, there is thus a certain amount of ambiguity since an increase in normalization can be compensated for by an increase in slope. This degeneracy is only present in the studied experimental region where the fission barriers extend out to large distortions. In less stable regions, where the fission penetration only involves smaller distortions, the calculated half-lives will depend more on the normalization than on the slope. This feature obviously gives rise to large uncertainties in the predictions for nuclei with less extended barriers.

One hint as to which part of the mentioned (k, c) valley is the most appropriate one is provided by the isomeric half-lives. The isomeric fission tests a more limited part of deformation space as it only explores the second barrier region and this serves to favor one solution. In Fig. 5 we have included some calculated (with $k = 11.5$ and $c = 1.0$) and experimental isomeric half-lifes.[27-29] For the calculated isomeric half-lives there is a pronounced erroneous trend in going from U through Pu to Cm. For the two measured U isomers (^{236,228}U) the calculated values are around five orders of magnitude too long. This may indicate that the second barriers of these isotopes are too large. One should notice that for ^{234}U the calculated value is of the same order as the two experimental numbers for ^{236,238}U. For Pu the overall agreement is fairly good but the isotopic variation is in error. This may reflect the sensitivity to the more detailed structure of the second barrier, which we treat here in a rather crude manner. Finally, the calculated values for ^{242,244}Cm come out around seven orders of magnitude too short as compared with experiment. The similar calculations with $k = 6.5$ and $c = 0.5$ yield isomeric half-lives which are one to two orders of magnitude longer [this change can be estimated on the basis of Fig. 4 and Eq. (8)]. Although the present results for the isomeric half-lives are far from satisfactory, the results do seem to point in favor of the irrotational-type slope, i.e., a value of the slope parameter c not far from unity. In the following discussion we have only considered the macroscopic-type inertial-mass function with $k = 11.5$ and $c = 1.0$.

2. *Microscopic inertias*

Similarly, for the microscopic inertial-mass functions the renormalization factor ρ is determined by fitting to experiment. The optimum fit obtains for $\rho = 0.80$, corresponding to $\Delta = 1.3$, which is a factor of around twenty. One should thus note that the microscopic calculations with one overall normalization factor leads to a fit which is as good as that obtained with two parameters in the case of a macroscopic-type inertial function. Figure 6 shows the corresponding results for the spontaneous-fission half-lives. Also in this figure we have included isomeric half-lives. (As both the potential V and the inertia B are originally calculated in terms of the ϵ coordinate it may appear more natural in the microscopic case to carry through the calculations in terms of ϵ. This has been done and leads to an almost equally good fit, the differences being largest for the nuclei with very extended barriers.)

As can be seen from Figs. 5 and 6, the different sets of effective inertial-mass functions lead to rather similar results for the calculated fission half-lives. The similarity of the discrepancies with the data to a large part appear to reflect inaccuracies in the common effective barrier potentials employed. Below we shall point out some of the sources of error.

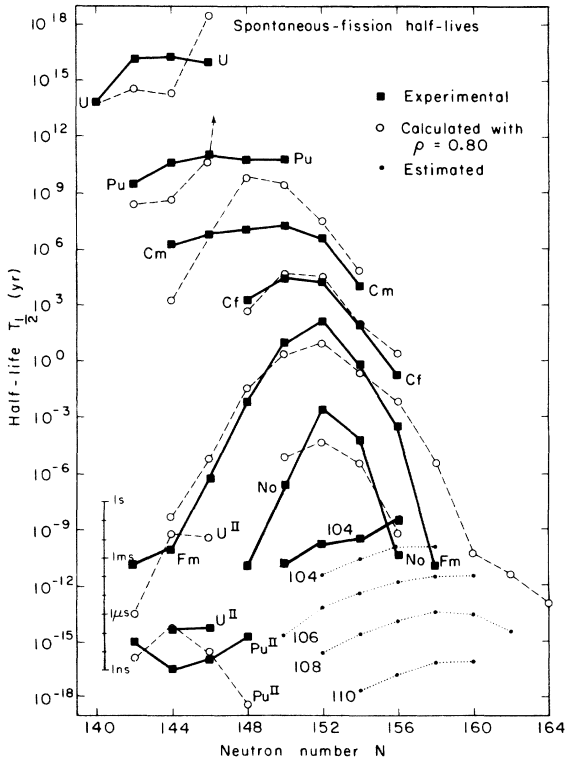

FIG. 6. Spontaneous-fission half-lives calculated with the microscopic inertial-mass functions having $\rho = 0.80$. Similar to Fig. 5.

One problem associated with the construction of the fission barrier potentials arises from the fact that the available deformation energy surfaces only extend out to deformations with $\epsilon = 1.0$. For the lighter elements (U, Pu, and Cm) the fission penetration explores larger deformations. Moreover, for some isotopes of U and Pu the second barrier region has been found theoretically[14,15] to have a double-hump structure; this further complicates the situation for these nuclei. These difficulties, in combination with the additional problem of ascertaining the effective fission path beyond the last saddle point, gives rise to a rather poor accuracy for the outer barriers of these nuclei.

The problem of extrapolating the barrier potential beyond $\epsilon = 1.0$ becomes particularly difficult for the two isotopes ^{242,244}Pu. The emerging barrier is by far too extended. These two isotopes have therefore not been included in the fit. A similar problem arises also for the elements U and Cm but to a more moderate extent, as can be seen from the half-life plots in Figs. 5 and 6.

Another problem associated with the theoretical fission barrier potentials is connected with the shell effect occurring at neutron number $N = 152$. Experimentally,[23,24,30] it is found that the ground-state mass corrections in this region exhibit a pronounced minimum at $N = 152$ for Fm and No isotopes. This effect is only in part reproduced in the calculations. Consequently, the calculated half-lives are expected to exhibit a less pronounced peak around this neutron number than is observed experimentally. This effect is clearly seen in Figs. 5 and 6.

A delicate theoretical problem arises from the interplay between the ground-state shell correction and the second barrier height for the elements from Fm and beyond. This problem is not special to the modified-oscillator model. The same critical situation occurs when the folded-Yukawa model is employed for the calculation of the deformation energies.[15]

As was already pointed out in Ref. 1, the sinking of the second barrier below the ground-state energy (including the 0.5 MeV vibrational energy) leads to a drastic decrease of the fission half-life (up to a factor of 10^5) due to the sudden and appreciable decrease in the amount of barrier that needs to be penetrated. Theoretically this effect occurs for fermium at $N = 160$, whereas the drastic experimental drop occurs at $N = 158$. This may suggest that the variation of the calculated ground-state energy is too gentle. This also seems to be the case for nobelium. The calculated half-lives exhibit a too smooth behavior around $N = 152$, but if, as an example, the difference between the mass corrections for the two isotopes ^{252}No and ^{254}No is taken from experiment, the ratio of the calculated half-lives comes out in agreement with experiment.

The problem remains present also for heavier elements as is discussed below.

To remedy this situation various effects have been investigated, such as a redetermination of the parameters κ and μ in the $A \approx 255$ region and a consideration of particle-number-fluctuation corrections in the BCS wave function; they are found to be of minor significance. The inclusion of nonisotropic pairing, as yet untried, may reduce this discrepancy.

In concluding this part we remark that the two types of inertial-mass function lead to rather similar results on the whole, for the region of nuclei considered. The microscopic-type inertia gives the best reproduction of the half-life data, namely a mean factor of error of around 20. This set of inertial functions is associated with less ambiguity and it is probably better suited for predictions concerning more distant nuclei (for example, it takes into account possible local shell-structure effects in the inertial mass).

B. Stability predictions

We turn now to the question of predicting the new stability properties of so far unobserved heavy and superheavy nuclei.

1. Transactinide elements

We have made preliminary estimates of the spontaneous-fission and α decay half-lives for the elements with Z between 104 and 110. For this purpose we have estimated the fission barrier potentials by calculating the deformation energy in five deformation points fixed *a priori*. The first has $\epsilon = 0.23$ and $\epsilon_4 = 0.010$ and corresponds approximately to the ground state, judging from the systematics of the preceding elements. Similarly, the point ($\epsilon = 0.40$, $\epsilon_4 = -0.005$) is approximately the axially symmetric saddle point. The results for this point have been duly corrected for the effect of axial asymmetry. In addition to these two approximate extreme points three deformation points have been chosen along an approximate effective fission path: (0.45, 0.015), (0.55, 0.030), and (0.65, 0.080). The first of these lies close to the estimated saddle point and the γ corrections have also been applied there.

Of course, this prescription leads only to approximate barriers but we can hope to infer the over-all systematics of the half-lives. In Figs. 5 and 6 we have included the spontaneous-fission half-lives calculated with these estimated barrier potentials. The smooth behavior exhibited may in

part reflect the employed prescription.

Beyond nobelium the theoretical fission barriers have only one peak. Consequently, the calculated fission half-lives are relatively short (at most milliseconds) and, moreover, exhibit a smooth variation with neutron number. As follows from our remarks above, the existence of a shell at $N=152$ could drastically change this behavior in the neighborhood of that neutron number.

Taken at their face value, the present calculations indicate that the isotopes of the element 106 generally have spontaneous-fission half-lives which are shorter by a factor of around 30 than the 104 isotopes with the same neutron number. This suggests that even 106 isotopes may exist with a spontaneous-fission half-life not much shorter than that of ^{258}Fm. Because of the uncertainty arising from the discussed $N=152$ problem it is not possible to predict with confidence which neutron number will give the largest stability.

The calculated half-lives for the element 108 show the same trend as those for 106 but are generally a factor of around 10^2 shorter. The half-lives of the 110 isotopes are further reduced by a factor of 10^3, approximately.

For experimental guidance, we have also calculated the corresponding α-decay energies and half-lives, using the semiempirical formula of Taagepera and Nurmia.[31] The results are displayed in Table II. We have used the calculated[2] ground-state masses as well as the "estimated" masses obtained as described above on the basis of the first of the five fixed deformation points. The mismatch between the two sets of results reflects the large uncertainty associated with these estimates.

It appears that more accurate theoretical predictions for this particular region of nuclei cannot be made until more accurate deformation-energy surfaces have been established.

TABLE II. α decay energies and half-lives as obtained on the basis of the calculated ground-state minima (left columns) as well as on the basis of the "estimated" ground-state minima based on a deformation point fixed *a priori* (right columns). The kinetic energy of the α particle is denoted Q_α. The α half-life, $T_{1/2}$, is obtained by use of the semiempirical formula of Taagepera and Nurmia (Ref. 31).

Mother	Q_α (MeV)		$\log T_{1/2}$ (yr)	
^{252}No	8.46		−8.24	
^{254}No	8.66		−8.86	
^{258}No	8.53		−8.47	
^{258}No	8.66		−8.89	
^{256}104	9.75	8.59	−11.45	−8.00
^{258}104	9.63	8.70	−11.14	−8.38
^{260}104	9.43	8.69	−10.57	−8.34
^{262}104	8.41			−7.42
^{260}106	10.45	9.64	−12.70	−10.57
^{262}106	10.01	9.61	−11.59	−10.50
^{264}106	9.68	9.43	−10.69	−9.97
^{266}106		9.25		−9.45
^{260}108		10.45		−12.18
^{262}108		10.54		−12.39
^{264}108		10.49		−12.28
^{266}108		10.32		−11.83
^{268}108		10.15		−11.39
^{270}108		10.02		−11.06

2. *r-process region*

The nuclei in the r-process region are relatively short-lived and have a realatively narrow fission barrier. Hence, for these nuclei, the inclusion of the ϵ_4 dependence of the r coordinate can have a significant effect via the effective inertial-mass function. As the ϵ_4 dependence is most important for large distortions, we may for an estimate of the effect in the r-process region neglect the ϵ_4 shrinkage of the barriers. The effect on the half-lives is then due solely to the increase in the renormalization factor k or ρ and may be estimated by the following formula:

$$\delta \log T_{1/2} \approx \frac{1}{2}\frac{\delta B}{B}[20.5 + \log T_{1/2}\ (\text{sec})]\,. \tag{8}$$

For the macroscopic-type inertial-mass functions the relative increase in k is 15%. Thus, for a half-life of one second the predicted half-life should increase by $1\frac{1}{2}$ orders of magnitude.

3. *Superheavy elements*

In our previous calculations[26] of the spontaneous-fission half-lives for the superheavy elements the ϵ_4 dependence of the r coordinate was not included. As already discussed in Sec. II, a consistent inclusion will lead to longer half-life predictions for nuclei with less extended barriers. We have therefore reexamined the superheavy region, with the present more complete treatment.

On the whole, the resulting effect is small, particularly so for the most stable nuclei near the center of the superheavy island. For nuclei with half-lives of around one year the increase in the stability only amounts to less than half an order of magnitude. The general conclusions of our previous study in the superheavy region[26] are thus not significantly altered by the present investigation.

Note added in proof: Since the present paper was submitted new half-life data for the nucleides ^{242}Fm, ^{250}102, and $^{254\text{-}260}$104 have been reported in Ref. 32. These data points are added in the Figs. 5 and 6.

†Work performed under the auspices of the Energy Research and Development Administration.

*On leave from the University of Aarhus, Aarhus, Denmark.

[1]J. Randrup, C. F. Tsang, P. Möller, S. G. Nilsson, and S. E. Larsson, Nucl. Phys. A217, 221 (1973).

[2]S. E. Larsson, P. Möller, S. G. Nilsson, I. Ragnarsson, J. Randrup, and C. F. Tsang (unpublished).

[3]S. G. Nilsson, C. F. Tsang, A. Sobiczewski, Z. Szymanski, S. Wycech, C. Gustafson, I. L. Lamm, P. Möller, and B. Nilsson, Nucl. Phys. A131, 1 (1969).

[4]W. D. Myers and W. J. Swiatecki, Ann. Phys. (N. Y.) 84, 186 (1974).

[5]J. Randrup, Lawrence Berkeley Laboratory Report LBL-1699, 1973 (unpublished).

[6]V. M. Strutinsky, Nucl. Phys. A95, 420 (1967); A122, 1 (1968).

[7]J. Randrup, Lawrence Berkeley Laboratory Report LBL-2385, 1974 (unpublished).

[8]S. E. Larsson and G. Leander, in *Proceedings of the Third International Atomic Energy Agency Symposium on Physics and Chemistry of Fission, Rochester (1973)* (International Atomic Energy Agency, Vienna, 1974), p. 177.

[9]S. E. Larsson, P. Möller, and S. G. Nilsson, Phys. Scr. 10A, 53 (1974).

[10]G. Leander, Nucl. Phys. A219, 245 (1974).

[11]V. V. Pashkevich, Nucl. Phys. A169, 175 (1971).

[12]U. Götz, H. C. Pauli, and K. Junker, Phys. Lett. 39B, 436 (1972).

[13]S. E. Larsson (unpublished).

[14]P. Möller, Nucl. Phys. A192, 529 (1972).

[15]P. Möller and J. R. Nix, Nucl. Phys. A229, 269 (1974).

[16]E. O. Fiset and J. R. Nix, Nucl. Phys. A193, 647 (1972).

[17]S. G. Nilsson, S. E. Larsson, P. Möller, J. Randrup, K. Pomorski, A. Baran, and A. Sobiczewski (unpublished).

[18]L. Wilets, *Theories of Nuclear Fission* (Clarendon, Oxford, 1964).

[19]M. Brack, J. Damgaard, A. S. Jensen, H. C. Pauli, V. M. Strutinsky, and C. Y. Wong, Rev. Mod. Phys. 44, 320 (1972).

[20]D. R. Bés, K. Dan. Vidensk. Selsk. Mat. Fys. Medd. 33, No. 2 (1961).

[21]A. Sobiczewski, Z. Szymański, S. Wycech, S. G. Nilsson, J. R. Nix, C. F. Tsang, C. Gustafson, P. Möller, and B. Nilsson, Nucl. Phys. A131, 67 (1969).

[22]K. Pomorski (unpublished).

[23]Yu. Ts. Oganessian, A. G. Demin, and A. S. Iljinov, JINR report, Dubna, 1974 (unpublished).

[24]K. Hulet, E. Hyde, R. Vandenbosch, V. Viola, and S. V. Jackson, private communications.

[25]A. Ghiorso, in *Proceedings of the Robert A. Welch Foundation Conference on Chemical Research, Texas, 1969* (Robert A. Welch Foundation, Houston, Texas, 1970), Vol. XIII, p. 109.

[26]J. Randrup, S. E. Larsson, P. Möller, A. Sobiczewski, and A. Łukasiak, Phys. Scr. 10A, 60 (1974).

[27]H. J. Specht, Phys. Scr. 10A, 21 (1974).

[28]V. Metag, E. Liukkonen, O. Glomset, and A. Bergman, in *Proceedings of the Third International Atomic Energy Agency Symposium on Physics and Chemistry of Fission, Rochester, 1973* (International Atomic Energy Agency, Vienna, 1974), p. 317.

[29]H. C. Britt, At. Data Nucl. Data Tables 12, 407 (1973).

[30]A. H. Wapstra and N. B. Gove, At. Data Nucl. Data Tables 9, 267 (1971).

[31]B. Taagepera, M. Nurmia, Ann. Acad. Sci. Fennicae 78, 1 (1961), Sec. A. VI.

[32]V. I. Chepigin, G. N. Flerov, A. S. Iljinov, Yu. Ts. Oganessian, O. A. Orlova, G. S. Popeko, B. V. Shilov, G. M. Ter-Akopyan, and S. P. Tretyakova, JINR Report No. E15-9064, Dubna, 1975 (unpublished).